Phosphorylation-Induced Distance Change in a Cardiac Muscle Troponin I Mutant†

Wen-Ji Dong,‡ Murali Chandra,§ Jun Xing,‡ Mingda She,‡ R. John Solaro,§ and Herbert C. Cheung*,‡

Department of Biochemistry and Molecular Genetics, University of Alabama at Birmingham, Birmingham, Alabama 35294-2041, and Department of Physiology and Biophysics, College of Medicine, University of Illinois at Chicago, Chicago, Illinois 60612

Received September 3, 1996; Revised Manuscript Received December 16, 1996⊗

ABSTRACT: Phosphorylation of two adjacent serine residues in the unique N-terminal extension of cardiac muscle troponin I (cTnI) is known to decrease the Ca^{2+}-sensitivity of cardiac myofilaments. To probe the structural significance of the N-terminal extension, we have constructed two cTnI mutants each containing a single cysteine: (1) a full-length cTnI mutant (S5C/C81I/C98S) and (2) a truncated cTnI mutant (S9C/C50I/C67S) in which the N-terminal 32 amino acid residues were deleted. We determined the apparent binding constants for the complex formation between IAANS-labeled cardiac troponin C (cTnC) and the two cTnI mutants. The affinities of the cTnC for the truncated cTnI mutant were: (1) 1.5×10^6 M^{-1} in EGTA, (2) 28.9×10^6 M^{-1} in Mg^{2+}, and (3) 87.5×10^6 M^{-1} in $Mg^{2+} + Ca^{2+}$. These binding constants were approximately 1.4-fold smaller than the corresponding values obtained with the full-length cTnI mutant, suggesting a very small contribution of the N-terminal extension to the binding of cTnI to cTnC. Cys-5 in the full-length cTnI mutant was labeled with IAANS, and the distribution of the separation between this site and Trp-192 was determined by analysis of the efficiency of fluorescence resonance energy transfer from Trp-192 to IAANS. The following mean distances were obtained with the unphosphorylated full-length mutant: 44.4 Å (cTnI alone), 48.3 Å (cTnI + cTnC), 46.3 Å (cTnI + cTnC in Mg^{2+}), and 51.6 Å (cTnI + cTnC in $Mg^{2+} + Ca^{2+}$). The corresponding values of the mean distance determined with the phosphorylated full-length cTnI mutant were 35.8, 36.6, 34.8, and 37.3 Å. The phosphorylation of cTnI reduced the half-width of the distribution from 9.5 to 3.7 Å. Similar but less pronounced decreases of the half-widths were also observed with the phosphorylated cTnI complexed with cTnC in different ionic conditions. Thus, phosphorylation of cTnI resulted in a decrease of 9−12 Å in the mean distance between the sites located at the N- and C-terminal portion of cTnI. Our results indicate that phosphorylation elicits a change in the conformation of cTnI which underlies the basis of the phosphorylation-induced modulation of cTnI activity.

Troponin I, one of the three subunits of the troponin complex that regulates muscle contraction, exists as a unique variant in heart muscle. The isoforms of TnI from skeletal and cardiac muscle are very similar in their amino acid sequences except that the cardiac isoform contains an additional 32-residue N-terminal extension. As with skeletal muscle TnI, cTnI inhibits the actomyosin ATPase activity in relaxed muscle. Upon binding of Ca^{2+} to the low-affinity regulatory site of cTnC, the inhibition is removed as a result of altered interactions among the troponin subunits, actin, and tropomyosin. Clues as to how the N-terminal segment may alter these basic functional properties of cTnI have come from studies showing that the N-terminal segment can be phosphorylated by PKA *in vivo* and *in vitro* at the two adjacent serines (Ser-23 and Ser-24). Several lines of evidence indicate that the phosphorylation of these two serines may have a unique and important regulatory role in modulating cardiac function (Solaro, 1986). For example, this phosphorylation appears responsible for a reduced apparent Ca^{2+}-affinity of cardiac troponin (Robertson et al., 1982) associated with PKA dependent phosphorylation of cardiac myofilaments.

The structural changes occurring with phosphorylation and responsible for the altered activity of cTnI are not clear. However, there is evidence that phosphorylation induces a new structural state of cTnI, whereas, the N-terminal extension itself does not affect cTnI activity. The truncated recombinant cTnI in which the N-terminal extension was absent retained the biological activity in a manner similar to native cTnI (Guo et al., 1994). Moreover, Wattanapermpool et al. (1995) demonstrated that the unique N-terminal extension of cTnI altered myofibrillar ATPase activity only when the segment was phosphorylated. Al-Hillawi et al. (1995) reported that, compared to a phosphorylated analogue, unphosphorylated cTnI bound more strongly to actin. They also showed that the unphosphorylated cTnI bound more strongly to cTnC than the phosphorylated form. There is some evidence on the structural changes in the N-terminal extension of the cTnI molecule induced by PKA phospho-

† This work was supported by NIH Grants HL52508 (H.C.C.) and HL49934 (R.J.S.) and by Postdoctoral Fellowships from the Muscular Dystrophy Association to W.-J.D. and from the American Heart Association of Metropolitan Chicago to M.C.

* Corresponding author Tel: (205) 934-2485. FAX: (205) 975-4621. E-mail: hccheung@bmg.bhs.uab.edu.

‡ University of Alabama at Birmingham.

§ University of Illinois at Chicago.

⊗ Abstract published in *Advance ACS Abstracts,* May 15, 1997.

[1] Abbreviations: TnI, troponin I; TnC, troponin C; cTnI, troponin I from cardiac muscle; cTnC, troponin C from cardiac muscle; cTnI/NH_2, truncated cTnI mutant (S9C/C50I/C67S) in which the first 32 residues were deleted; PCR, polymerase chain reaction; IAANS, 2-[(4′-iodoacetamido)anilino]naphthalene-6-sulfonic acid; DTT, dithiothreitol; EGTA, ethylene glycol bis(β-aminoethyl ether)-*N,N,N′,N′*-tetraacetic acid; MOPS, 3-(*N*-morpholino)propanesulfonic acid; FRET, fluorescence resonance energy transfer; PKA, protein kinase A.

S0006-2960(96)02227-1 CCC: $14.00

rylation, but how these changes are transmitted to the rest of cTnI and to cTnC is unknown. A fluorescence anisotropy study of the single tryptophanyl residue of cTnI indicated that phosphorylation resulted in a more compact hydrodynamic shape of the protein (Liao et al., 1992). Our spectral study of an extrinsic fluorescent probe linked to Cys-5 in the full-length cTnI mutant indicated that phosphorylation induced substantial conformational changes in the N-terminal segment (Dong et al., 1997).

In the present study, we report results from FRET experiments showing that phosphorylation decreases the distance between Cys-5 and Trp-192 by 9−12 Å. The present results provide the first direct evidence of a phosphorylation-induced folding of the N-terminal extension toward the C-terminus of cTnI.

MATERIALS AND METHODS

Isolation of cTnI/NH_2(S9C/C50I/C67S). The cTnI mutant (S5C/C81I/C98S) plasmid DNA (Dong et al., 1997) was subjected to PCR using the following oligonucleotides as primers. The forward primer (primer 1: 5′GCCTATGCCATGGAGCCACACGCCAAGAAAAAGTGCAAGATCTCCGCC3′) was designed to incorporate codons for amino acids 33−44 of the full-length cTnI (underlined) and a change in codon at position 40 (this corresponds to position 9 in the truncated mutant) to substitute Ser with Cys. This was preceded on the 5′ side by nucleotides of the pET3d vector (Novagen) including the *Ned*I restriction enzyme site. Nucleotide sequence of the reverse primer (primer 2: 5′GGTGTCTGGATCC**TCA**GCCCTCAAACTTTTTCTTG3′) corresponded to the noncoding strand of the cTnI gene which included codons for amino acids 206−211 (underlined). This was flanked on the 5′ end side by a stop codon (in bold) and the *Bam*HI restriction enzyme site. The PCR product containing the cTnI/NH_2(S9C/C50I/C67S) DNA fragment was digested with *Nco*I and *Bam*HI and ligated into the pET3d expression vector (Novagen). The plasmid DNA carrying the insert was sequenced to verify the mutation. Expression and purification of cTnI were as previously described (Guo et al., 1994).

Phosphorylation of Cardiac Muscle TnI Mutants. The full-length cTnI mutant (S5C/C81I/C98S) was obtained as described previously (Dong et al., 1997). The mutant was phosphorylated at pH 7.0 and 30 °C, using 125 units of the catalytic subunits of PKA/mg of cTnI in a medium containing 50 mM KH_2PO_4, 10 mM $MgCl_2$, 0.5 mM EGTA, and 5 mM DTT. The reaction was initiated with the addition of ATP to a final concentration of 0.5 mM. The mixture was incubated at 30 °C for 20 min, followed by exhaustive dialysis at 4 °C against the basic buffer (30 mM MOPS at pH 7.0, 1 mM EGTA, 0.3 M KCl, and 0.5 mM DTT). Mutant cTnI/NH_2(S9C/C50I/C67S) was similarly treated with PKA.

Fluorescent Labeling of Native cTnC and cTnI Mutants. Native cTnC was prepared from bovine heart as previously described (Dong & Cheung, 1996). Its two sulfhydryl groups (Cys-35 and Cys-84) were labeled with IAANS by the general procedure described in the preceding paper (Dong et al., 1997). Cys-5 in the full-length cTnI mutant and the single cysteine in the truncated mutant, cTnI/NH_2(S9C/C50I/C67S), were also labeled with IAANS as previously described (Dong et al., 1997). When the effect of phosphorylation was studied with cTnI mutants, labeling was done with samples that had been pretreated with PKA. A given PKA-treated protein was first thoroughly dialyzed against 0.1 mM DTT in the basic buffer. The sulfhydryl-reduced protein was further dialyzed against the basic buffer in which DTT was omitted. The dialyzed protein was reacted with a 3-fold molar excess of IAANS in the presence of 6 M urea at 4 °C for 10 h. The reaction was terminated with a 3−5-fold molar excess of DTT, and the solution was exhaustively dialyzed against the basic buffer containing 6 M urea to remove unreacted fluorophore. A further dialysis against the basic buffer in the absence of urea was repeated three times. A turbidimetric tannin micromethod (Mejbaum-Katzenellenbogen & Dobryszcka, 1959) or the Bradford method (Bradford, 1976) was used to determine the concentration of the labeled proteins. The amounts of label covalently attached to the proteins were determined by absorbance, using a molar extinction coefficient of 24 000 M^{-1} cm^{-1} at 325 nm (Johnson et al., 1980). The degree of labeling was 1.8−2.0 for cTnC and was >0.9 for the two cTnI mutants.

Fluorescence Measurements. Steady-state spectral measurements were carried out at 20 ± 0.1 °C on an SLM 8000C spectrofluorometer as previously described (Dong et al., 1997). The measurements of the fluorescence intensity decay and anisotropy decay of the single tryptophan in cTnI mutants were carried out at 20 °C on a PRA single photon-counting system (model 3000), using a Rhodamine 6G dye laser synchronously pumped by a mode-locked argon ion laser (Spectra Physics, model 171). The mode-locker operated at 41 MHz. The cavity-dumped dye laser was set at 4 MHz and provided a train of light pulses with a 15 ps full width at half-maximum height (FWHM). The output of the dye laser was frequency-doubled to 295 nm by an angle-tuned KDP crystal (Spectral Physics, model 390) to generate UV picosecond pulses with tunable frequency from 290 to 310 nm. The laser intensity was attenuated by neutral density filters to reduce the sample counting rate down to <3 kHz to avoid photon pileup. The wavelength of the tryptophan emission excited with 295 nm pulses was isolated with a Ditric three-cavity 334-nm interference filter or selected with a 4-nm band pass monochromator (Instruments SA, Inc.). The photon-counting system used a Hamamatsu R955 PM tube and had a response time of about 500 ps in FWHM. A DCM [(4-(dicyanomethylene)-2-methyl-6-(*p*-dimethylaminostyryl)-4*H*-pyran] dye laser was used to generate picosecond pulses at 325 nm for excitation of IAANS as previously described (Dong et al., 1997). The procedures previously described (Dong et al., 1997) were used for measurements and analyses of the intensity decays and anisotropy decays of tryptophan and IAANS.

Binding of cTnI Mutant to cTnC. The binding of cTnC to the two mutants of cTnI was determined using cTnC labeled with IAANS as previously described (Liao et al., 1994). In a typical experiment, a fixed concentration of IAANS-labeled cTnC was titrated with unphosphorylated or phosphorylated cTnI mutant, and the change in the IAANS fluorescence intensity was used to monitor the extent of binding.

Determination of Intersite Distances. The distance between the donor site (Trp-192) and the acceptor site (IAANS-labeled Cys-5) was determined from the distribution of the distances between the donor and acceptor, using time-domain

lifetime data obtained from unlabeled and labeled cTnI mutant. The theory for measurements of FRET to determine distance distributions has been previously described (Lakowicz et al., 1988; Cheung et al., 1991). We summarize the time-domain procedures used in the present analysis. In the present case, the intensity decay of the donor (Trp) is not monoexponential, and the analysis of the donor-alone decay is given by the multiexponential model

$$I_D(t) = \sum_i \alpha_{D_i} \exp(-t/\tau_{D_i}) \quad (1)$$

where α_{D_i} are the fractional amplitudes associated with the decay times τ_{D_i} for the donor. In the presence of the Förster-type of resonance energy transfer, the intensity decay of a donor−acceptor pair separated by a unique distance r is given by

$$I_{DA}(r,t) = \sum_{i=1} \alpha_{D_i} \exp\left[-\frac{t}{\tau_{D_i}} - \frac{t}{\tau_{D_i}}\left(\frac{R_o}{r}\right)^6\right] \quad (2)$$

where R_o is the Förster critical distance at which the transfer efficiency is 0.5. The observed decay of an ensemble of donor−acceptor pairs is given by

$$I_{DA}(t) = \int_0^\infty P(r) I_{DA}(r,t)\, dr \quad (3)$$

It is assumed here that R_o is the same for each donor−acceptor pair. $P(r)$ is the probability distribution of distances and is assumed to be a Gaussian

$$P(r) = \frac{1}{Z}\frac{1}{\sigma\sqrt{2\pi}} \exp\left[-{}^1/_2\left(\frac{r-\bar{r}}{\sigma}\right)^2\right] dr \quad (4)$$

where $\bar{r}$ is the mean distance and σ is the standard deviation of the distribution. The half-width (hw) of the distribution is given by hw = 2.3544σ. In practice the integration limits in eq 3 are not from $-\infty$ to ∞, and the integral is calculated over a range of distances from r(min) to r(max) with the lower limit being about 5 Å. $P(r)$ is normalized by the area, and Z is the normalization factor.

The Förster distance R_o was calculated from the spectral properties of the donor and acceptor fluorophores:

$$R_o = (8.79 \times 10^{-5}) n^{-4} Q\kappa^2 J \qquad (\text{in Å}^6) \quad (5)$$

where n is the refractive index of the solution and was taken as 1.4, Q is the donor quantum yield, κ^2 is the orientation factor, and J is the spectral overlap integral and is given by

$$J = \frac{\int F_d(\lambda)\, \epsilon_a(\lambda) \lambda^4\, d\lambda}{\int F_d(\lambda)\, d\lambda} \quad (6)$$

where $F_d(\lambda)$ is the fluorescence intensity of the donor at wavelength λ and $\epsilon_a(\lambda)$ is the molar absorption of the acceptor at λ. The overlap integral was calculated by numerical integration.

RESULTS

Interaction of cTnC with cTnI Mutants. cTnC labeled with IAANS was previously used to monitor the interaction between cTnC and native cTnI (Liao et al., 1994). The same method was used to probe the interaction between cTnC and the two cTnI mutants. Binding curves for the interaction of cTnC with the full-length cTnI mutant obtained under different conditions are shown in Figure 1. When the ionic conditions were changed from EGTA to either Mg^{2+} or Mg^{2+} plus Ca^{2+}, these curves were shifted toward lower free cTnI concentrations. The apparent binding constant was 2.1×10^6 M^{-1} in the presence of EGTA and increased by a factor of 19 in the presence of Mg^{2+}. A further 3-fold enhancement in the binding affinity was observed when Ca^{2+} was present in addition to Mg^{2+}. However, the phosphorylation of cTnI decreased the overall affinity for cTnC under all conditions tested (Table 1). The affinity of cTnC for the full-length cTnI mutant determined in the presence of Mg^{2+} or Mg^{2+} plus Ca^{2+} was in good agreement with the previously reported data for native cTnI (Liao et al., 1994). When the ionic medium was changed from Mg^{2+} to Ca^{2+}, the cTnI·

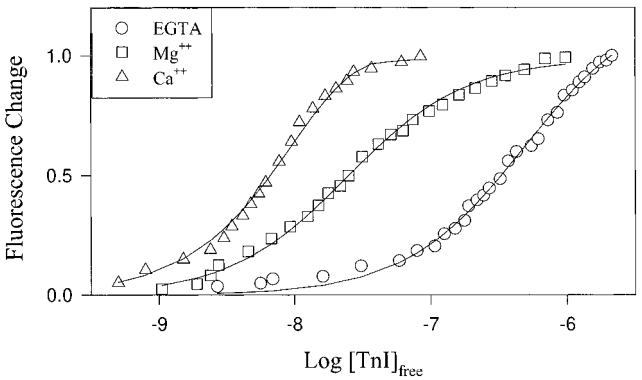

FIGURE 1: Titration of IAANS-labeled cTnC with full-length cTnI mutant (S5C/C81I/C98S) in different ionic conditions. The change in fluorescence intensity is plotted against the logarithm of free cTnI concentration. The measurements were carried out in 0.3 M KCl, 30 mM MOPS at pH 7.0, 0.5 mM DTT, and 1 mM EGTA at 20 °C. Circle, in EGTA (cTnC concentration was 3×10^{-7} M^{-1}); square, in 3 mM Mg^{2+} (cTnC concentration was 1.0×10^{-7} M^{-1}); triangle, in 2 mM Ca^{2+} (cTnC concentration was 5×10^{-8} M^{-1}). The data were fitted to the equation $y = \{nK[x]/(1 + K[x])\}$, where y is the fractional change in fluorescence intensity, K is the apparent binding constant, n is the number of binding sites, and $[x]$ is the free cTnI concentration. An interactive nonlinear least-squares procedure (Gauss−Newton algorithm) was used to estimate K and n. The recovered parameters are summarized in Table 1.

Table 1: Binding Parameters for the Complex Formation of IAANS-Labeled cTnC with cTnI Mutants[a]

complex	condition	$K \times 10^{-6}$ (M^{-1})	n	$-\Delta G°$ (kcal/mol)
cTnI·cTnC	EGTA	2.1 ± 0.1	1.20 ± 0.02	8.5
	Mg^{2+}	40.5 ± 0.1	0.99 ± 0.01	10.2
	Ca^{2+}	120.1 ± 2.6	1.10 ± 0.02	10.9
p-cTnI·cTnC	EGTA	0.55 ± 0.02	1.30 ± 0.02	7.7
	Mg^{2+}	21.5 ± 0.2	0.86 ± 0.02	9.9
	Ca^{2+}	50.4 ± 0.9	1.18 ± 0.07	10.4
cTnI/NH_2·cTnC	EGTA	1.5 ± 0.1	1.15 ± 0.01	8.3
	Mg^{2+}	28.9 ± 1.0	0.96 ± 0.01	10.0
	Ca^{2+}	87.5 ± 2.5	1.20 ± 0.02	10.7

[a] cTnI is mutant cTnI(S5C/C81I/C98S), and p-cTnI is the PKA phosphorylated cTnI mutant. cTnI/NH_2 is the truncated mutant cTnI/NH_2(S9C/C50I/C67S). cTnC is cardiac TnC labeled with IAANS. The conditions for these experiments are given in Figure 1. The values of the apparent binding constant K and the number of binding sites (n) were recovered from the data shown in Figure 1. These values are given as the mean ± standard deviation of the best-fitted values obtained from several preparations. The free energy values were calculated from the standard relationship $\Delta G° = -RT \ln K$, with the temperature at 20 °C.

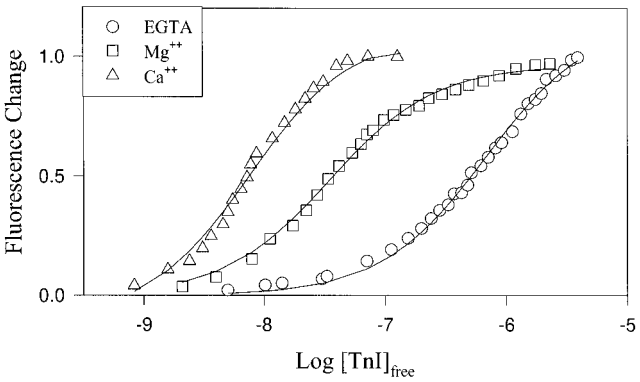

FIGURE 2: Titration of IAANS-labeled cTnC with the truncated cTnI mutant (S9C/C50I/C67S) in different ionic conditions. Circle, in EGTA; square, in 3 mM Mg^{2+}; and triangle, in 2 mM Ca^{2+}. Other conditions were the same as for Figure 1.

cTnC complex was stabilized by 0.7 kcal/mol in the absence of phosphorylation and by 0.5 kcal/mol when cTnI was phosphorylated (Table 1). These coupling free energy values are essentially the same as those reported for the native cTnI. However, when tested in the presence of EGTA the observed apparent affinity of cTnC for either the unphosphorylated or phosphorylated cTnI mutant was 7−10-fold weaker than that reported for native cTnI (Liao et al., 1994). The reason for this decreased affinity is not clear, but from evidence discussed above it is clear that, in the presence of Mg^{2+} or Ca^{2+}, the cTnI mutant and native cTnI have very similar cTnC binding properties.

We also studied the interaction of IAANS-labeled cTnC with the truncated cTnI mutant (S9C/C50I/C67S). Binding curves obtained under different conditions are shown in Figure 2. The binding constants determined from these fitted curves were intermediate between those obtained with the unphosphorylated and phosphorylated full-length cTnI mutant. The extent of Mg^{2+}- or Ca^{2+}-induced enhancement in the binding of the truncated cTnI mutant to cTnC was identical to that observed for the interaction between the full-length cTnI mutant and cTnC.

Intensity Decays of Donor Trp-192. Figure 3 compares the intensity decay of Trp-192 in the cTnI mutant with the decay determined in the presence of the acceptor IAANS attached to Cys-5. The donor-alone decay (Figure 3b) followed a triexponential decay law with three lifetimes, and the intensity-weighted mean lifetime was 3.53 ns. The decay of the donor in the presence of the acceptor was also triexponential and faster (Figure 3c), with a mean lifetime of 3.33 ns. This was an indication of energy transfer from the donor to the acceptor. The donor-alone decay (data not shown) of the phosphorylated cTnI mutant was essentially unaltered (mean lifetime = 3.52 ns). In the acceptor-labeled phosphorylated cTnI mutant, the mean lifetime was reduced to 2.96 ns. These data are summarized in Table 2. Additional measurements were made on the intensity decays of Trp-192 with unlabeled and labeled cTnI mutant complexed with cTnC in the presence of Mg^{2+} and Mg^{2+} plus Ca^{2+}. In each case, the decay was triexponential and the cTnI phosphorylation resulted in a decrease in the mean lifetime. Qualitatively, these lifetime data provided an initial indication of energy transfer between Trp-192 and Cys-5 and showed that the transfer in the phosphorylated samples was enhanced.

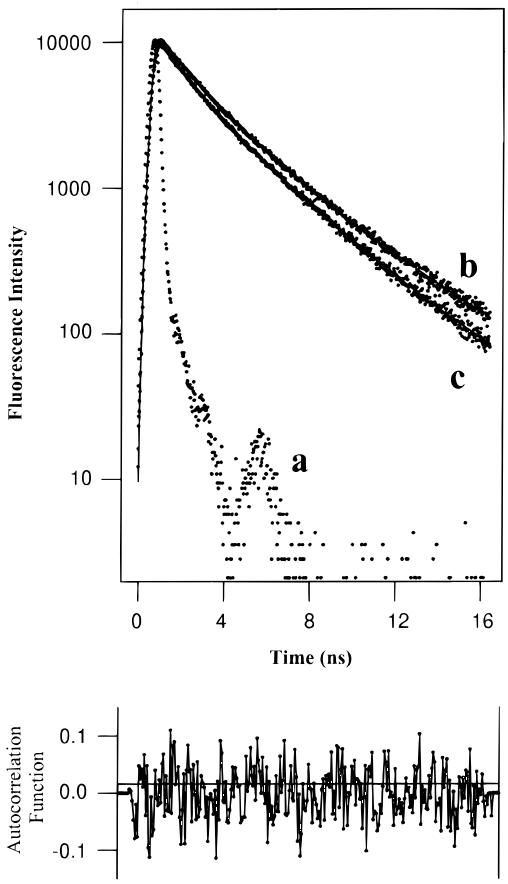

FIGURE 3: Representative fluorescence intensity decay plots of the single tryptophan Trp-192 in the full-length cTnI mutant (S5C/S81I/C98S). Curve a is the laser profile, curve b is the decay of Trp-192 in the absence of an energy acceptor, and curve c is the Trp-192 decay in the presence of the acceptor IAANS attached to Cys-5. Both sets of data were fitted with a triexponential function. The lower panel is the autocorrelation function of the residuals for the fit shown in b.

Table 2: Intensity Decay of Trp-192 in Mutant cTnI(S5C/C81I/C98S)

sample	τ_i (ns)	α_i	$\langle\tau\rangle$ (ns)	χ^2_R (ns)	D−W
cTnI (D)[a]	5.84	0.14	3.53	1.02	2.09
	2.81	0.57			
	1.10	0.29			
cTnI (D + A)	4.18	0.21	3.33	1.11	1.93
	1.69	0.22			
	0.07	0.57			
p-cTnI (D)	5.63	0.17	3.52	1.17	1.97
	2.77	0.53			
	1.20	0.31			
p-cTnI (D + A)	3.70	0.40	2.96	1.12	2.09
	1.51	0.47			
	1.43	0.14			

[a] D indicates donor-alone (unlabeled) full-length cTnI mutant (S5C/C81I/C98S), and (D + A) indicates the IAANS-labeled full-length cTnI mutant containing both donor and acceptor. p-cTnI is the phosphorylated cTnI mutant. These decay data were fitted with a triexponential function, with lifetimes τ_i and the associated fractional amplitudes α_i. $\langle\tau\rangle$ is the intensity-weighted mean lifetime calculated from $\langle\tau\rangle = \sum\alpha_i\tau_i^2/\sum\alpha_i\tau_i$. Protein concentration was ~2 μM, and measurements were made in the basic buffer at 20 °C. The standard errors were in the range 0.04−0.07 ns for τ_1 (the longest component), 0.02−0.04 ns for τ_2, and 0.01−0.02 ns for τ_3 (shortest component) for all samples. The corresponding errors were 0.01−0.04 for α_1, 0.01−0.05 for α_2, and 0.01−0.04 for α_3.

Anisotropy Decays of Donor Trp-192 and Acceptor IAANS Attached to Cys-5. The anisotropy decays of Trp-192 in the

Table 3: Limiting Anisotropy and Axial Depolarization Factor of Trp-192 and IAANS Linked to Cys-5 in cTnI Mutant (S5C/C81I/C98S)[a]

sample	anisotropy		depolarization factor	
	Trp	IAANS	$\langle d^x_D \rangle$	$\langle d^x_A \rangle$
cTnI	0.114	0.287	0.689	0.933
cTnI·cTnC	0.085	0.296	0.595	0.947
cTnI·cTnC + Mg^{2+}	0.082	0.272	0.585	0.908
cTnI·cTnC + Ca^{2+}	0.087	0.277	0.060	0.916
p-cTnI	0.144	0.310	0.689	0.969
p-cTnI·cTnC	0.110	0.329	0.667	0.998
p-cTnI·cTnC + Mg^{2+}	0.124	0.313	0.719	0.974
p-cTnI·cTnC + Ca^{2+}	0.122	0.309	0.713	0.968

[a] $\langle d^x_D \rangle$ and $\langle d^x_A \rangle$ denote the axial depolarization factors of donor and acceptor, respectively, and were calculated from the observed anisotropy and the fundamental anisotropy of the fluorophores (Dale et al., 1979). cTnI is the full-length cTnI mutant, p-cTnI is the PKA phosphorylated cTnI mutant, and cTnC is native cardiac TnC. For measurements of the limiting anisotropy of Trp-192, the measurements were made with the unlabeled mutant either in the absence of cTnC or in the presence of a large excess of cTnC (cTnI·cTnC and p-cTnI·cTnC). The measurements were made in the basic buffer at 20 °C with cTnI concentration ~5 μM. The Ca^{2+} concentration was 2 mM.

full-length cTnI mutant were determined for the unphosphorylated and phosphorylated forms and for the two cTnI species complexed with cTnC. The decay in each case was adequately fitted to a biexponential function, yielding two rotational correlation times (results not shown), in agreement with previous results obtained with native cTnI (Liao et al., 1992). The fast correlation time was in the range of 1 ns or less and reflected motion of the indole ring. The other parameter of interest in the present study was the limiting anisotropy r_o, which was used to calculate the axial depolarization factor of the donor ($\langle d^x_D \rangle$). These two parameters are summarized in Table 3. The anisotropy decays of the acceptor IAANS attached to Cys-5 were previously reported (Dong et al., 1997). Also summarized in Table 3 are the values of r_o and the axial depolarization factor ($\langle d^x_A \rangle$) for the acceptor.

Distribution of Donor−Acceptor Distances in the Full-length cTnI Mutant. The distribution of the distances between Trp-192 and Cys-5 was calculated from the intensity decay data by assuming a Gaussian (eq 3). The results are summarized in Table 4. The recovered distributions for the unphosphorylated and phosphorylated cTnI mutant are shown in Figure 4A. The two striking results were that the phosphorylation sharpened the distribution and shifted it to smaller distances. The half-width was decreased by a factor of 2.5 (5.8 Å), and the mean distance was reduced by 8.6 Å. The two fits were satisfactory as judged from the χ^2_R values (Table 4) and the residuals and the autocorrelation of the residuals (results not shown). To further evaluate whether these data do indicate differences between the two preparations, we compared the uncertainties in the distance and the half-width by calculating the variance ratio surfaces shown in Figure 4B and 4C. These surfaces are quite steep and do not intersect. It is clear that the two distributions are distinct from each other. We refitted the cTnI data by fixing the hw at 7 Å and obtained a 4-fold increase in the χ^2_R value (Table 4). The residuals and the autocorrelation of the residuals for this second fit showed large and nonrandom fluctuations (results not shown), indicating that the fit was not acceptable. When the hw was fixed at the value (4 Å) recovered from the phosphorylated cTnI sample,

Table 4: Intersite Distance Distribution between Trp-192 and IAANS Attached to Cys-5 in the Mutant cTnI(S5C/C81I/C98S)[a]

sample	R_o (Å)	$\bar{r}$ (Å)	hw (Å)	χ^2_R
cTnI	24.3	44.4	9.5	1.07
			(7)	4.2
			(4)	49.8
p-cTnI	24.8	35.8	3.7	1.1
			(6)	1.5
			(9)	3.7
cTnI·cTnC	24.6	48.3	8.1	1.0
			(6)	5.7
			(9)	3.7
p-cTnI·cTnC	25.5	36.6	6.0	1.0
			(8)	21.4
c-TnI·cTnC + Mg^{2+}	24.8	46.8	10.4	1.2
			(6)	21.4
p-cTnI·cTnC + Mg^{2+}	24.3	34.8	5.2	1.2
			(9)	3.2
c-TnI·cTnC + Ca^{2+}	24.3	51.5	11.1	1.1
			(7)	3.9
p-cTnI·cTnC + Ca^{2+}	24.6	39.3	6.6	1.0
			(11)	2.7

[a] R_o is the Förster distance, $\bar{r}$ is the mean distance, and hw is the half-width of the distribution. The distribution parameters were calculated using $\kappa^2 = {}^2/_3$. The value of the hw given in parentheses indicates that the hw was held fixed at the indicated value during the least-squares analysis. cTnI concentration was ~2 μM. Notations for samples and other conditions were the same as given in Table 3.

a 50-fold increase in the χ^2_R value was obtained. Similarly, when the data for the phosphorylated sample were refitted by holding the hw at 6 and 9 Å, the χ^2_R values were elevated and the autocorrelations of the residuals were nonrandom, further indicating poor fits. These results show that the data were adequate to demonstrate significantly different mean distances and half-widths for the two forms of the cTnI mutant.

When the IAANS-labeled cTnI mutant was complexed with cTnC, the mean intersite distance was increased by 4 Å to 48.3 Å, while the hw was decreased by 1.5 Å to 8.1 Å (Table 4). The phosphorylation reduced the mean distance within the complex by over 11 Å to 36.6 Å. Although the phosphorylation also decreased the hw as for uncomplexed p-cTnI, the reduction was only 2 Å. When the data for cTnI·cTnC were refitted by holding the hw at the value (6 Å) recovered for p-cTnI·cTnC, the χ^2_R was increased 5-fold; reciprocally, when the hw for p-cTnI·cTnC was fixed at the value (8 Å) recovered for cTnI·cTnC, the χ^2_R value was 4-fold increased. These results indicate that the two distributions for cTnI·cTnC and p-cTnI·cTnC are distinct from each other. Mg^{2+} had only small effects on the distributions recovered from the binary protein complex, regardless of whether the cTnI mutant was unphosphorylated or phosphorylated. In each case, the mean distance was slightly smaller (<2 Å) than the distance for the apo complex and the hw was within 1−2 Å of that recovered in the absence of Mg^{2+}. When the medium was changed from one containing only Mg^{2+} to one containing both Mg^{2+} and Ca^{2+}, the distribution was shifted to larger distances with the mean distance increasing from 46.8 to 51.6 Å and the hw increasing by <1 Å. The phosphorylation of the cTnI mutant in the binary protein complex containing bound Ca^{2+} resulted in a significantly different distribution. The mean distance was reduced by 12.2 Å to 39.3 Å, whereas the hw was reduced by 4.5 Å. That these two distributions can be considered distinct from each other is supported by a 3−4-fold increase

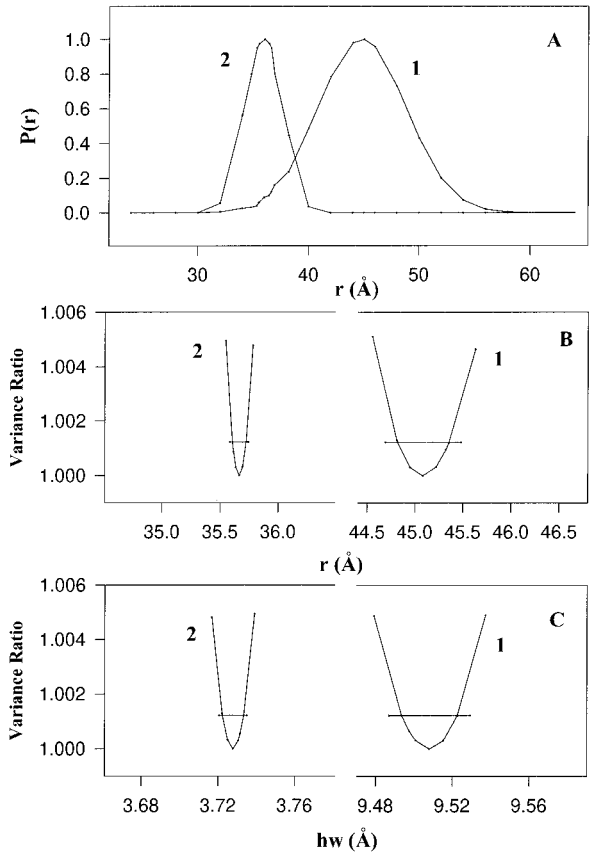

FIGURE 4: Analysis of FRET data for the distance between Trp-192 and Cys-5 in the full-length cTnI mutant (S5C/C81I/C98S). (A) Distributions of the distances in the unphosphorylated cTnI mutant (curve 1) and the phosphorylated mutant (curve 2). A value of $\kappa^2 = {}^2/_3$ was used in these calculations. Since the degree of acceptor labeling was less than stoichiometric, the observed intensity decay of the donor in the acceptor-labeled protein contained a contribution from those Trp-192 residues which did not participate in energy transfer. A correction for this was incorporated into the analysis program. (B) Dependence of the variance ratio (χ^2_R) on the mean distance ($\bar{r}$) of the distributions from cTnI (curve 1) and p-cTnI (curve 2). The value of $\bar{r}$ was held constant at the value indicated on the horizontal axis, and the hw was varied to minimize χ^2_R. (C) Dependence of the variance ratio on the hw (half-width) of the distributions from cTnI (curve 1) and p-cTnI (curve 2). In B and C, the values of the variance ratio are normalized to the minimum value. The horizontal lines indicate the statistically significant increase in the variance ratio at an approximately 67% confidence level using the F-statistic. The analysis was carried out with the SFS_LS/GAUDIS program written by Dr. Michael L. Johnson. This program allows for variance space that is nonlinear and asymmetrical.

in the χ^2_R value when each set of the data was refitted using the same value of the hw recovered for the other set of data. Taken together, the analysis of the distributions of the distances indicates that the phosphorylation resulted in a large decrease in the mean separation between Trp-192 and Cys-5 in the cTnI mutant either uncomplexed or complexed with cTnC. This decrease of the mean distance was accompanied by a narrowing of the distribution of the distances.

Distribution of Donor−Acceptor Distances in Truncated cTnI Mutant. The distributions of the distances between Trp-161 and Cys-9 in the truncated mutant cTnI/NH_2(S9C/C50I/C67S) were calculated from the intensity decays of the Trp-161 in the uncomplexed mutant and the mutant complexed with cTnC, in the absence of divalent cations and the presence of Mg^{2+} and Mg^{2+} plus Ca^{2+}. In this mutant, Trp-161 corresponds to Trp-192 and Cys-9 corresponds to residue 40 in the full-length cTnI. The mean distances and half-widths of the distributions from these calculations are summarized in Table 5. The recovered mean distance in the truncated mutant was 35.5 Å, with a half-width of 7.7 Å. Upon complexation with cTnC, $\bar{r}$ increased to 39.4 Å and the hw increased to 9.7 Å. The values of $\bar{r}$ and hw were little affected by the presence of divalent cations. The three distributions obtained from the binary protein complex were essentially indistinguishable from one another by the criteria used to distinguish the distributions recovered from the full-length cTnI mutant. More importantly, these distributions were not affected by prior treatment of the truncated cTnI mutant with PKA (data not shown).

Table 5: Intersite Distance Distribution between Trp-161 and IAANS Attached to Cys-9 in the Truncated Mutant cTnI/NH_2(S9C/C50I/C67S)[a]

sample	$\bar{r}$ (Å)	hw (Å)	χ^2_R
cTnI/NH_2	35.5	7.7	1.2
cTnI/NH_2·cTnC	39.4	9.7	1.0
cTnI/NH_2·cTnC + Mg^{2+}	38.9	9.3	1.0
cTnI/NH_2·cTnC + Ca^{2+}	40.2	9.6	1.1

[a] Conditions were the same as given for Table 4.

DISCUSSION

In the preceding paper (Dong et al., 1997), we showed that PKA-dependent phosphorylation of a full-length cTnI mutant (S5C/C81I/C98S) resulted in extensive changes in the fluorescence of IAANS covalently attached to Cys-5. These phosphorylation-induced changes were indicative of a folding in the N-terminal extension of cTnI. In the present study, we extend these observations and provide evidence to show that the phosphorylation of cTnI leads to a decrease in the distance between Cys-5 and Trp-192, a further indication of the phosphorylation-induced folding of the N-terminal segment.

The present results support the conclusion from a previous study (Guo et al., 1994) that the unique N-terminal extension of cTnI does not itself play a role in the Ca^{2+} activation process. If the N-terminal extension is not involved in the interaction between the cTnI and cTnC, one would expect very small or no differences in the binding constant between full-length and truncated cTnI for cTnC. This appears to be the case as the difference between the two sets of binding constants are less than 30%. More importantly, cTnC has about the same affinity for both the full-length and truncated cTnI mutant in the presence of Mg^{2+} and has a higher, but also very similar, affinity for both mutants in the presence of Ca^{2+}. Very similar coupling free energies are obtained for the binding of Ca^{2+} and either the full-length or the truncated cTnI mutant to cTnC. Treatment of the truncated mutant with PKA has no effect on the binding constant indicating that the observed phosphorylation effect on the binding constant is due to the phosphorylation of Ser-23 and Ser-24.

We have analyzed the data from energy transfer between Trp-192 and IAANS attached to Cys-5 in terms of a distribution of the donor−acceptor distances. The various statistics used in our analysis clearly demonstrate distinct distributions of the distances for the unphosphorylated and phosphorylated cTnI mutant. The recovered distributions are apparent distributions in that they are influenced by the

Förster critical distance R_o of the specific donor−acceptor pair, the orientations of the donor and acceptor fluorophores and their motions, conformational fluctuations, and site-to-site diffusion. In particular, a distribution of the orientation factor (κ^2) can contribute to the overall observed apparent distance distribution. No theoretical models are available to describe the distribution of separation between two sites in the native conformation of proteins. However, recent simulation studies (Wu & Brand, 1992) have provided a basis to consider several factors that can modify an apparent distribution of intersite distances. The mean distance can be obtained reliably if R_o is smaller than the mean distance, irrespective of the other factors (Wu & Brand, 1992). This condition is met for the systems studied in the present work. Since our main concern is the difference in the mean distance between two states of the cTnI mutant, the experimental conditions used are optimal for this purpose. If a single value of the orientation factor κ^2 is used in data analysis, the apparent distribution width recovered from eq 3 may contain contribution from real distance distribution and from static orientation. The "true" distance distribution width would be smaller than the apparent width even for the case $R_o < \bar{r}$. The angular rotations of donor and acceptor due to Brownian motion can narrow down the distribution of orientation and, therefore, reduce the width of the apparent distance distribution. The effect of this motional averaging will depend upon the orientational rate in comparison with the rate of energy transfer. Probe motions on the order of 10 ps or faster in rotational correlation time will make a negligible contribution to the recovered distance distribution width, but slower correlation time may contribute to the apparent width. The correlation times of both the indole ring of Trp-192 and the IAANS attached to Cys-5 are on the order of 0.2−1 ns (Liao et al., 1992; Dong et al., 1997). These motions may contribute to the observed 9.5 Å half-width of the distribution for the unphosphorylated cTnI mutant. This half-width is reduced to 3.7 Å upon phosphorylation. This reduction is not likely a result of enhanced motional averaging of the donor and acceptor because their correlation times in p-cTnI remain the in the 0.1−1 ns range. We used $\kappa^2 = {}^2/_3$ to calculate the distance distribution. A factor that could contribute to the observed narrowing of the distribution width would be a phosphorylation-induced change in κ^2 due to a change in the static orientation of the probes. The potential contribution of the orientation factor can be estimated from the axial depolarization factors of the donor and acceptor. For the unphosphorylated cTnI, $\langle d^x_D \rangle = 0.689$ and $\langle d^x_A \rangle = 0.933$. The corresponding values for p-cTnI are 0.689 and 0.969, respectively. These depolarization factors are essentially the same for both forms of the cTnI mutant and indicate the same upper and lower limits of the orientation contribution to the apparent distance distributions for both samples. These considerations suggest that much of the observed 5.8 Å decrease in the apparent half-width could be due to a decrease of the real distance distribution. Physically, if the segment of the cTnI peptide between the donor and acceptor sites is held more rigidly, the end-to-end distribution is expected to become narrower (Lakowicz et al., 1988).

Whether an intersite separation will display a distribution can be assessed, independently of the analysis using eq 3, from the average lifetimes of the donor calculated using the multiexponential model (eq 1). Two types of average lifetime can be calculated from the individual lifetimes and the associated amplitudes. The intensity-weighted lifetimes ($\langle\tau\rangle$) for several samples are listed in Table 2. The amplitude-weighted lifetime is given by $\bar{\tau} = \sum\alpha_i\tau_i$. If there is a single value of the donor−acceptor separation, the ratio $A = \langle\tau\rangle_{DA}/\langle\tau\rangle_D$ and the ratio $B = \bar{\tau}_{DA}/\bar{\tau}_D$ should be equal. If $A/B > 1$, a distance distribution is indicated (Albaugh et al., 1989). The value of A/B is 2.5 for the cTnI mutant and reduced to 0.98 for p-cTnI. These results indicate a distribution of distances for the cTnI, but a negligible distribution width for p-cTnI. The theoretical value of A/B does not include the effects of any distribution of probe orientation. The small observed distribution width for p-cTnI may be indicative of an orientational effect. Importantly, the values of the A/B ratio range from 1.2 to 1.5 for the unphosphorylated mutant complexed with cTnC regardless of the absence or presence of Mg^{2+} or Ca^{2+}, indicative of distance distributions. The corresponding A/B values for the phosphorylated cTnI in the complex are reduced to 0.98−0.95, suggesting relatively sharp or even no distributions in the distances as for the uncomplexed cTnI. These results of the A/B ratio provide further insights into the observed apparent distributions. Taken together, the FRET results lead to the conclusion that both the mean distance and the half-width of the distribution are significantly reduced upon the phosphorylation. This decrease in the mean distance is carried over to the binary complex formed between the cTnI mutant and cTnC. The distribution of the donor−acceptor distances between Trp-161 and Cys-9 labeled with IAANS in the truncated mutant is not affected by prior treatment of the mutant with PKA. We have previously shown that there are no PKA sites in cTnI other than those in the amino terminal extension and that there is no PKA dependent phosphorylation of the truncated mutant (Noland et al., 1995; Wattanapermool et al., 1995). Thus, it is the phosphorylation of sites in the amino terminal extension that is responsible for the observed decrease in the mean distance between Cys-5 and Trp-192.

Our FRET results provide clues as to the mechanisms by which phosphorylation of cTnI alters Ca^{2+} regulation of myofilament activity. Data presented here and in the previous report (Dong et al., 1997) provide strong support for the idea that the phosphorylation-induced folding of the N-terminal extension towards the C-terminal end of cTnI underlies the molecular basis of alterations in the activity of cTnI. It appears that the folding may alter contact between cTnI and cTnC and may be responsible for the diminished affinity of phosphorylated cTnI for cTnC (Liao et al., 1994). Indeed there is evidence from ^{31}P NMR studies demonstrating that the N-terminal phosphorylated residues in cTnI experience a more acidic environment when complexed with cTnC (Al-Hillawi et al., 1995). The molecular mechanism by which the phosphorylation induces a folding of the N-terminal segment is not yet fully understood. However, Liao et al. (1992) suggested that electrostatic interactions of a cluster of arginine side chains at positions 20, 21, 22, and 28 with phosphate groups at positions 23 and 24 may play a role in this conformational change. Supporting evidence for this suggestion comes from the observation that phosphorylation effects can be mimicked by simply substituting Ser-23 and Ser-24 with acidic amino acids (Dohet et al., 1996). This shows that electrostatic interactions could play

a critical role in the phosphorylation-induced folding of the N-terminal extension.

In summary, our observations indicate that the unique N-terminal extension of cTnI does not play a major role in the binding of cTnI to cTnC. On the other hand, PKA-induced phosphorylation of cTnI results in a folding of this N-terminal extension leading to a decrease in the distance between Cys-5 and Trp-192. This conformational change may provide the structural basis for the phosphorylation-induced modulation of cTnI activity.

ACKNOWLEDGMENT

We thank Dr. Michael M. Johnson of the University of Virginia for the statistical package CFS_LS, which was used in the analysis of the distribution of distances, and for assistance in the analysis. This package was written for the Center for Fluorescence Spectroscopy at the University of Maryland School of Medicine.

REFERENCES

Albaugh, S., Lan, J., & Steiner, R. F. (1989) *Biophys. Chem. 33*, 71−76.

Al-Hillawi, E., Bhandar, D. G., Trayer, H. R., & Trayer, I. P. (1995) *Eur. J. Biochem. 228*, 962−970.

Bradford, M. M. (1976) *Anal. Biochem. 71*, 248−254.

Cheung, H. C.,Wang, C.-K., Gryczynski, I., Wiczk, W., Laczko, G., Johnson, M. L., & Lakowicz, J. R. (1991) *Biochemistry 30*, 5238−5247.

Dale, R. F., Eisinger, J., & Blumberg, W. E. (1979) *Biophys. J. 26*, 161−194.

Dohet, C. Kogler, H., Al-Hillawi, E., Trayer, I. P., & Rüegg, J. C. (1994) *Biophys. J. 70*, A328.

Dong, W.-J., & Cheung, H. C. (1996) *Biochim. Biophys. Acta 1295*, 139−146.

Dong, W.-J., Chandra, M., Xing, Jun, Solaro, R. J., & Cheung, H. C. (1997) *Biochemistry 36*, 6745−6753.

Guo, X., Wattanapermpool, J., Palmiter, K. A., Murphy, A. M., & Solaro, R. J. (1994) *J. Biol. Chem.* 269, 15210−15216.

Johnson, J. D., Collins, J. H., Robertson, S. P., & Potter, J. D. (1980) *J. Biol. Chem. 255*, 9635−9640.

Lakowicz, J. R., Gryczynski, I., Cheung, H. C., Wang, C.-K., Johnson, M. L., & Joshi, N. (1988) *Biochemistry 27*, 9149−9160.

Liao, R., Wang, C.-K., & Cheung, H. C. (1992) *Biophys. J. 63*, 986−995.

Liao, R., Wang, C.-K., & Cheung, H. C. (1994) *Biochemistry 33*, 12729−12734.

Mejbaum-Katzenellenbogen, W., & Dobryszcka, W. M. (1959) *Clin. Chim. Acta 4*, 515−520.

Noland, T. A., Guo, Raynor, R. I., Averyhart-Fullard, V., Jideama, N. M., Solaro, R. J., & Kuo, J. F. (1995) *J. Biol. Chem. 43*, 25445−25454.

Robertson, S. P., Johnson, J. D., Holroyde, M. J., Kranias, E. G., Potter, J. D., & Solaro, R. J. (1982) *J. Biol. Chem. 257*, 260−263.

Solaro, R. J., Ed. (1986) in *Protein Phosphorylation in the Heart Muscle*, pp 129−156, CRC Press Inc., Boca Raton, FL.

Solaro, R. J., Moir, A. J. G., & Perry, A. V. (1976) *Nature 262*, 615−617.

Swiderek, K., Jaquet, K., Meyer, H. E., & Heilmeyer, L. M. G., Jr. (1988) *Eur. J. Biochem. 176*, 335−342.

Wang, C.-K., & Cheung, H. C. (1986) *J. Mol. Biol. 191*, 509−521.

Wattanapermpool, J., Guo, X., & Solaro, R. J. (1995) *J. Mol. Cell Cardiol. 27*, 1383−1391.

Wu, P., & Brand L. (1992) *Biochemistry 31*, 7939−7947.

BI9622276